Available online at www.sciencedirect.com
ScienceDirect
International Journal of Solids and Structures 45 (2008) 3192–3202
INTERNATIONAL JOURNAL OF SOLIDS AND STRUCTURES
www.elsevier.com/locate/ijsolstr

Modal localization in mistuned tube-array structures

Bo-Wun Huang [a,*], Huang-Kuang Kung [a], Jao-Hwa Kuang [b]

[a] Department of Mechanical Engineering, Cheng Shiu University, Kaohsiung, Taiwan, ROC
[b] Department of Mechanical and Electromechanical Engineering, National Sun Yat-Sen University, Kaohsiung, Taiwan, ROC

Received 27 July 2007; received in revised form 4 January 2008
Available online 26 January 2008

Abstract

An investigation of mode localization in mistuned tube-array structures is studied in this work. The continuous action of hot-cold fluid shock waves in tube-array heat exchangers results in a significant abrasive wear of the tubes, which in turn alters their dynamic behavior and may introduce an undesirable modal localization effect within the tube bundle. This study performs a numerical investigation into the problem of modal localization in mistuned tube-array heat exchangers, with cross-flow. In conducting the investigation, the heat exchanger is modeled as a bundle of periodically-arranged cooling tubes in which the vibrational displacements of the individual tubes are weakly coupled to those of their neighbors via a squeezed water film in the gap between them. In general, the numerical results reveal that damage to even a single tube within the array is sufficient to introduce a severe modal localization effect. Furthermore, due to the weak coupling effect of the fluid, the vibrational energy induced by modal localization is confined to the defected tube and its immediate neighbors, and hence the risk of further wear defected within the tube bundle is increased. The results suggest that the modal localization phenomenon is alleviated at higher values of the cross-flow velocity, but becomes more severe as the tube wall thickness is increased.

Keywords: Mode localization; Mistuned system; Cross-flow; Periodic structure

1. Introduction

It has been reported that local structural defects or material irregularities in weakly-coupled periodic structures such as the tube bundles deployed in heat exchangers may generate an undesirable modal localization effect in which a strong low-frequency response is induced within the mistuned system Kuang and Huang (1999, 2001). The weak nature of the coupling between the tubes in the bundle confines the vibrational energy induced by the localization effect to the defected tube and those in its immediate neighborhood. This vibration confinement effect accelerates the formation of defects in the neighboring tubes and, in severe cases, may lead to the catastrophic failure of the entire structure. The modal localization effect is particularly acute in large-scale tube bundles such as those used in the tube-array heat exchangers. In the heat exchanger, abrasion

* Corresponding author. Fax: +886 7 7310213.
E-mail address: huangbw@csu.edu.tw (B.-W. Huang).

0020-7683/$ - see front matter © 2008 Elsevier Ltd. All rights reserved.
doi:10.1016/j.ijsolstr.2008.01.019

defects are commonly formed near the center of the tubes due to impact friction and wear during operation. Such abrasions are common in heat exchange systems operated under severe conditions Kuang and Tsai (1987, 1988) and Yetisir et al. (1998). However, their presence is clearly undesirable in critical cooling systems such as those used in nuclear power plants. Consequently, when designing heat exchange systems, an essential task is to establish the conditions under which the modal localization effect is induced such that these conditions can be specifically avoided in the design and/or operational stages.

The problem of modal localization has been extensively investigated in various engineering and industrial contexts, including cracked disk assemblies, large space structures, general assemblies with cyclic symmetry, coupled circular plates, and so on Huang and Kuang (2001), Bendiksen (1987), Wei and Pierre (1988) and Orgun (1994)]. Various aspects of heat exchange systems have also been investigated in the literature, including their heat transfer and pressure-loss properties Kwak et al. (2002) and their dynamic response and vibration damping characteristics Lorenzini and Giuliani (2002), Eisinger et al. (1996), Taylor et al. (1998). However, the specific problem of modal localization in heat exchangers in cross-flow has not been addressed. In Katinas and Perednis (1991), Papp and Chen (1994), Longatte et al. (2003), Zhu et al. (1994), Zhu et al. (1997), Weaver and Lover (1977), Weaver and Korogannakis, 1983 and Price et al. (1987), the authors demonstrated that the flow of fluid in and around the tubes in a heat exchanger has a significant effect on the vibration and instability characteristics of the system. Therefore, when assessing the potential for the structural failure of heat exchange systems, it is necessary to consider not only the modal localization effect induced by local defects and material irregularities, but also the effects of the cross-flow fluid itself.

Accordingly, the current study conducts a numerical investigation into the problem of modal localization in a periodically-arranged, weakly-coupled tube bundle in a principal component cooling water heat exchange system in cross-flow. The respective effects of the cross-flow characteristics and the presence of a local defect on the dynamic response of the tube bundle are systematically examined. The investigations focus specifically on the formation and effects of modal localization within the tube bundle. For simplicity, the tubes are approximated as hollow Euler-Bernoulli beams with a round cross section. The weak coupling between the individual tubes in the bundle is implemented using the fluid stiffness model presented in Zhu et al. (1994), Zhu et al. (1997). Finally, the discrete modal localization equation for the mistuned heat exchange system is derived using Galerkin's method.

2. Equations of motion of coupled tube array

Fig. 1 presents a schematic illustration of the cross-flow type heat exchange system considered in the current study. The fluid enters the tube bundle with an average flow velocity U and generates a weak coupling between adjacent tubes in the bundle via the formation of a squeezed fluid film between them. As shown in Fig. 2(a), the tubes are assumed to be simply-supported at either end and to have a length L. Moreover, the outer diameter and wall thickness of each tube are denoted by D and b, respectively. The periodic arrangement of the tube bundle is shown schematically in Fig. 2(b). The tubes are arranged in accordance with a pitch-to-diameter

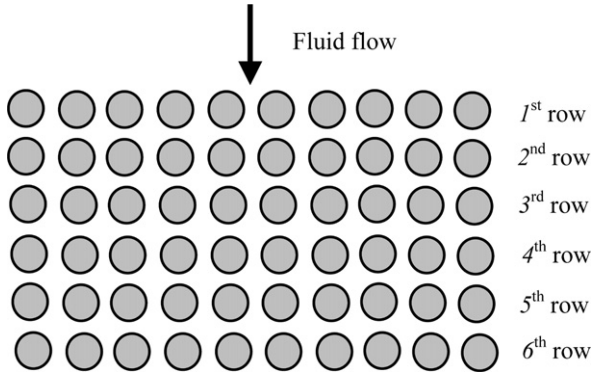

Fig. 1. Schematic illustration of periodically-arranged tube bundle in heat exchange system.

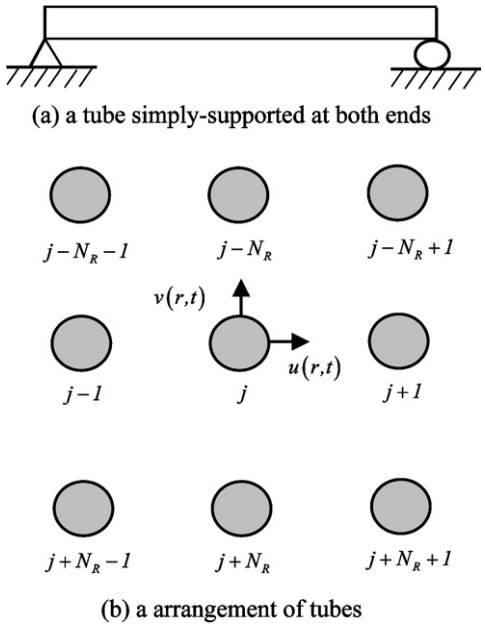

Fig. 2. Boundary conditions and geometrical arrangement of tubes in bundle.

ratio of 1.35. The notations, $v_j(r,t)$ and $u_j(r,t)$, denote the transverse flexible deflections of the jth tube in the horizontal and the perpendicular planes, respectively, as shown in Fig. 2(b).

According to Zhu et al. (1997), the equations of motion of the heat exchanger tubes have the form

$$E_j I_j \frac{\partial^4 u_j}{\partial r^4} + c_j \frac{\partial u_j}{\partial t} + m_j \frac{\partial^2 u_j}{\partial t^2} = g_j \tag{1a}$$

$$E_j I_j \frac{\partial^4 v_j}{\partial r^4} + c_j \frac{\partial v_j}{\partial t} + m_j \frac{\partial^2 v_j}{\partial t^2} = h_j \tag{1b}$$

for $j = 1, 2, 3, \ldots, N$, where E_j is the Young's modulus, I_j is the moment of area, and m_j, c_j, g_j and h_j are the mass, damping coefficient and fluid force components in the u and v directions, respectively, for the jth tube. The two fluid force components can be derived as

$$g_j = -\rho\pi R^2 \sum_{k=1}^{N} \left(\alpha_{jk} \frac{\partial^2 u_k}{\partial t^2} + \sigma_{jk} \frac{\partial^2 v_k}{\partial t^2} \right) + \frac{\rho U^2}{\omega_t} \sum_{k=1}^{N} \left(\alpha'_{jk} \frac{\partial u_k}{\partial t} + \sigma'_{jk} \frac{\partial v_k}{\partial t} \right) + \rho U^2 \sum_{k=1}^{N} \left(\alpha''_{jk} u_k + \sigma''_{jk} v_k \right), \tag{2a}$$

$$h_j = -\rho\pi R^2 \sum_{k=1}^{N} \left(\tau_{jk} \frac{\partial^2 u_k}{\partial t^2} + \beta_{jk} \frac{\partial^2 v_k}{\partial t^2} \right) + \frac{\rho U^2}{\omega_t} \sum_{k=1}^{N} \left(\tau'_{jk} \frac{\partial u_k}{\partial t} + \beta'_{jk} \frac{\partial v_k}{\partial t} \right), + \rho U^2 \sum_{k=1}^{N} \left(\tau''_{jk} u_k + \beta''_{jk} v_k \right) \tag{2b}$$

where ρ is the fluid density
R is the tube radius
t is time
ω_t is the circular frequency of the tube oscillations
U is the flow velocity
$\alpha_{jk}, \sigma_{jk}, \tau_{jk}, \beta_{jk}$ are the added fluid-mass coefficients
$\alpha'_{jk}, \sigma'_{jk}, \tau'_{jk}, \beta'_{jk}$ are the added fluid-damping coefficients
$\alpha''_{jk}, \sigma''_{jk}, \tau''_{jk}, \beta''_{jk}$ are the added fluid-stiffness coefficients

Equations (2a) and (2b) are cited from Zhu et al. (1997). In this article, the laminar flow is considered. As shown in Fig. 2, the fluid flows through the bundle in the u direction. Consequently, the effect of the transverse displacement component v_k on the exciting force components g_j and h_j is so small that it can be neglected, i.e., only the u displacement component must be considered. Hence, Eqs. (2a) and (2b) can be simplified to

$$g_j = -\rho\pi R^2 \sum_{k=1}^{N}\left(\alpha_{jk}\frac{\partial^2 u_k}{\partial t^2}\right) + \frac{\rho U^2}{\omega}\sum_{k=1}^{N}\left(\alpha'_{jk}\frac{\partial u_k}{\partial t}\right) + \rho U^2\sum_{k=1}^{N}(\alpha''_{jk}u_k), \tag{3a}$$

$$h_j = -\rho\pi R^2 \sum_{k=1}^{N}\left(\tau_{jk}\frac{\partial^2 u_k}{\partial t^2}\right) + \frac{\rho U^2}{\omega_t}\sum_{k=1}^{N}\left(\tau'_{jk}\frac{\partial u_k}{\partial t}\right) + \rho U^2\sum_{k=1}^{N}\left(\tau''_{jk}u_k\right). \tag{3b}$$

Due to the flow fluid introduced force, the jth tube would be excited by the force with components g_j and h_j from surround tubes. Consider all the tubes are vibrated harmonically with a frequency i.e. $u_k = \tilde{u}_k \cos\omega t$. Therefore, the fluid force components acting on the jth tube can be written as

$$g_j = \omega^2\rho\pi R^2\sum_{k=1}^{N}\alpha_{jk}\tilde{u}_k\cos\omega t - \rho U^2\sum_{k=1}^{N}\alpha'_{jk}\tilde{u}_k\sin\omega t + \rho U^2\sum_{k=1}^{N}\alpha''_{jk}\tilde{u}_k\cos\omega t, \tag{4a}$$

$$h_j = \omega^2\rho\pi R^2\sum_{k=1}^{N}\tau_{jk}\tilde{u}_k\cos\omega t - \rho U^2\sum_{k=1}^{N}\tau'_{jk}\tilde{u}_k\sin\omega t + \rho U^2\sum_{k=1}^{N}\tau''_{jk}\tilde{u}_k\cos\omega t. \tag{4b}$$

The equations of motion of the jth tube can then be rewritten as

$$E_jI_j\frac{\partial^4 u_j}{\partial r^4} + c_j\frac{\partial u_j}{\partial t} + m_j\frac{\partial^2 u_j}{\partial t^2} - \omega^2\rho\pi R^2\sum_{k=1}^{N}\alpha_{jk}\tilde{u}_k\cos\omega t + \rho U^2\sum_{k=1}^{N}\alpha'_{jk}\tilde{u}_k\sin\omega t - \rho U^2\sum_{k=1}^{N}\alpha''_{jk}\tilde{u}_k\cos\omega t = 0, \tag{5a}$$

$$E_jI_j\frac{\partial^4 v_j}{\partial r^4} + c_j\frac{\partial v_j}{\partial t} + m_j\frac{\partial^2 v_j}{\partial t^2} - \omega^2\rho\pi R^2\sum_{k=1}^{N}\tau_{jk}\tilde{u}_k\cos\omega t + \rho U^2\sum_{k=1}^{N}\tau'_{jk}\tilde{u}_k\sin\omega t - \rho U^2\sum_{k=1}^{N}\tau''_{jk}\tilde{u}_k\cos\omega t = 0. \tag{5b}$$

The boundary conditions for the jth tube are given by

$$u_j(0,t) = v_j(0,t) = 0, \quad u_j(L,t) = v_j(L,t) = 0, \quad \frac{\partial^2 u_j(0,t)}{\partial r^2} = \frac{\partial^2 v_j(0,t)}{\partial r^2} = 0, \quad \frac{\partial^2 u_j(L,t)}{\partial r^2} = \frac{\partial^2 v_j(L,t)}{\partial r^2} = 0. \tag{6}$$

The objective of the analysis performed in the current study is to investigate the effect of fluid coupling on the dynamics of the heat exchange system in general and on the introduction of modal localization in particular. According to Zhu et al. (1997), the fluid-damping coefficients are very small in stationary fluid. In this article, the fluid flow velocity is designed to be small. For simplicity, the damping effect induced by the fluid within the tube-array system is neglected. Hence the analysis considers only the coupling effects introduced by the jth tube's neighbors, i.e., tubes $(j-i)$, $(j+i)$, $(j+N_R)$ and $(j-N_R)$ (see Fig. 2(b)). Taking these coupling effects into account, the equations of motion of the jth tube can be re-formulated as

$$\begin{aligned} &E_jI_j\frac{\partial^4\tilde{u}_j}{\partial r^4} - \omega^2 m_j\tilde{u}_j - \omega^2\rho\pi R^2\sum_{k=1}^{N}\left(\alpha_{jj}\tilde{u}_j + \alpha_{jj-1}\tilde{u}_{j-1} + \alpha_{jj+1}\tilde{u}_{j+1} + \alpha_{jj+N_R}\tilde{u}_{j+N_R} + \alpha_{jj-N_R}\tilde{u}_{j-N_R}\right)\\ &\quad - \rho U^2\sum_{k=1}^{N}\left(\alpha''_{jj}\tilde{u}_j + \alpha''_{jj-1}\tilde{u}_{j-1} + \alpha'_{jj+1}\tilde{u}_{j+1} + \alpha''_{jj+N_R}\tilde{u}_{j+N_R} + \alpha''_{jj-N_R}\tilde{u}_{j-N_R}\right) = 0, \end{aligned} \tag{7a}$$

$$\begin{aligned} &E_jI_j\frac{\partial^4\tilde{v}_j}{\partial r^4} - \omega^2 m_j\tilde{v}_j - \omega^2\rho\pi R^2\sum_{k=1}^{N}\left(\tau_{jj}\tilde{u}_j + \tau_{jj-1}\tilde{u}_{j-1} + \tau_{jj+1}\tilde{u}_{j+1} + \tau_{jj+N_R}\tilde{u}_{j+N_R} + \tau_{jj-N_R}\tilde{u}_{j-N_R}\right)\\ &\quad - \rho U^2\sum_{k=1}^{N}\left(\tau''_{jj}\tilde{u}_j + \tau''_{jj-1}\tilde{u}_{j-1} + \tau''_{jj+1}\tilde{u}_{j+1} + \tau''_{jj+N_R}\tilde{u}_{j+N_R} + \tau''_{jj-N_R}\tilde{u}_{j-N_R}\right) = 0, \end{aligned} \tag{7b}$$

where N_R is the number of tubes in each row. The displacement sequence can be annotated in accordance with the arrangement of the tube array, i.e.,

$$u_{j-1}=0 \quad \text{if} \quad j-1<0,\ u_{j-1}=0 \quad \text{if} \quad j=nN_R+1, n=1,2,3,\ldots, \tag{8a}$$

$$u_{j+1}=0 \quad \text{if} \quad j+1>N,\ u_{j+1}=0 \quad \text{if} \quad j=nN_R, n=1,2,3,\ldots, \tag{8b}$$

$$u_{j-N_R}=0 \quad \text{if} \quad j-N_R<0,\ u_{j+N_R}=0 \quad \text{if} \quad j+N_R>N, \tag{8c}$$

where N and N_W denote the total number of tubes and the total number of rows in the tube array, respectively. For convenience, the following dimensionless parameters are introduced:

$$\bar{r}=\frac{r}{L}, \quad \bar{r}=0 \quad \text{to} \quad 1, \quad \bar{u}_j(\bar{r})=\frac{\tilde{u}_j(\bar{r})}{L}, \quad \bar{v}_j(\bar{r})=\frac{\tilde{v}_j(\bar{r})}{L}. \tag{9}$$

Eqs. (7a) and (7b) can then be rewritten as

$$\begin{aligned}&\gamma^2\frac{\partial^4\bar{u}_j}{\partial\bar{r}^4}-\omega^2\bar{u}_j-\omega^2\bar{m}_j^w\left(\alpha_{jj}\bar{u}_j+\alpha_{jj-1}\bar{u}_{j-1}+\alpha_{jj+1}\bar{u}_{j+1}+\alpha_{jj+N_R}\bar{u}_{j+N_R}+\alpha_{jj-N_R}\bar{u}_{j-N_R}\right)\\&\quad-\bar{k}_j^w\gamma^2\left(\alpha''_{jj}\bar{u}_j+\alpha''_{jj-1}\bar{u}_{j-1}+\alpha''_{jj+1}\bar{u}_{j+1}+\alpha''_{jj-N_R}\bar{u}_{j-N_R}+\alpha''_{jj+N_R}\bar{u}_{j+N_R}\right)=0,\end{aligned} \tag{10a}$$

$$\begin{aligned}&\gamma^2\frac{\partial^4\bar{v}_j}{\partial\bar{r}^4}-\omega^2\bar{v}_j-\omega^2\bar{m}_j^w\left(\tau_{jj}\bar{u}_j+\tau_{jj-1}\bar{u}_{j-1}+\tau_{jj+1}\bar{u}_{j+1}+\tau_{jj+N_R}\bar{u}_{j+N_R}+\tau_{jj-N_R}\bar{u}_{j-N_R}\right)\\&\quad-\bar{k}_j^w\gamma^2\left(\tau''_{jj}\bar{u}_j+\tau''_{jj-1}\bar{u}_{j-1}+\tau''_{jj+1}\bar{u}_{j+1}+\tau''_{jj-N_R}\bar{u}_{j-N_R}+\tau''_{jj+N_R}\bar{u}_{j+N_R}\right)=0,\end{aligned} \tag{10b}$$

where $\gamma=\sqrt{\frac{EI}{m_jL^4}}$, $\bar{m}_j^w=\frac{\rho\pi R^2}{m_j}$ and $\bar{k}_j^w=\frac{\rho U^2}{m_j\gamma^2}$. The parameters $\alpha_{ii}=1.0526, \alpha_{ij}=-0.2845, \alpha''_{ii}=-0.6, \alpha''_{ij}=0.5$, $\tau_{ii}=0, \tau_{ij}=0, \tau''_{ii}=-0.2$ and $\tau''_{ii}=-0.15$ are selected to study. The solutions for the above eigenvalue problem are assumed to have the forms

$$\bar{u}_j(\bar{r})\cos\omega t=\sum_{s=1}^{m}p_s^j(t)\phi_s^j(\bar{r}), \quad \bar{v}_j(\bar{r})\cos\omega t=\sum_{s=1}^{m}q_s^j(t)\phi_s^j(\bar{r}) \tag{11}$$

Using Galerkin's method, the equations of motion for the jth tube can be derived in matrix form as

$$\begin{aligned}&-\omega^2\left([m_j]^u+\left[\Lambda_j^j\right]^u\right)\{p\}_j+\gamma^2[k_j]^u\{p\}_j-\omega^2\left[\Lambda_{j-1}^j\right]^u\{p\}_{j-1}-\omega^2\left[\Lambda_{j+1}^j\right]^u\{p\}_{j+1}-\omega^2\left[\Lambda_{j-N_R}^j\right]^u\{p\}_{j-N_R}\\&\quad-\omega^2\left[\Lambda_{j+N_R}^j\right]^u\{p\}_{j+N_R}-\gamma^2\left[\Delta_{j-1}^j\right]^u\{p\}_{j-1}-\gamma^2\left[\Delta_{j+1}^j\right]^u\{p\}_{j+1}\\&\quad-\gamma^2\left[\Delta_{j-N_R}^j\right]^u\{p\}_{j-N_R}-\gamma^2\left[\Delta_{j+N_R}^j\right]^u\{p\}_{j+N_R}=0,\end{aligned} \tag{12a}$$

$$\begin{aligned}&-\omega^2\left([m_j]^v\{q\}_j+\left[\Pi_j^j\right]^{uv}\{p\}_j\right)+\gamma^2[k_j]^v\{q\}_j-\omega^2\left[\Pi_{j-1}^j\right]^{uv}\{p\}_{j-1}-\omega^2\left[\Pi_{j+1}^j\right]^{uv}\{p\}_{j+1}\\&\quad-\omega^2\left[\Pi_{j-N_R}^j\right]^{uv}\{p\}_{j-N_R}-\omega^2\left[\Pi_{j+N_R}^j\right]^{uv}\{p\}_{j+N_R}-\gamma^2\left[\Theta_{j-1}^j\right]^{uv}\{p\}_{j-1}\\&\quad-\gamma^2\left[\Theta_{j+1}^j\right]^{uv}\{p\}_{j+1}-\gamma^2\left[\Theta_{j-N_R}^j\right]^{uv}\{p\}_{j-N_R}-\gamma^2\left[\Theta_{j+N_R}^j\right]^{uv}\{p\}_{j+N_R}=0.\end{aligned} \tag{12b}$$

Eqs. (12a) and (12b) can be rearranged as

$$\begin{aligned}&-\omega^2\left([m]_j+[\Phi]_j^j\right)\begin{Bmatrix}p\\q\end{Bmatrix}_j+\gamma^2\left([k]_j-[\Psi]_j^j\right)\begin{Bmatrix}p\\q\end{Bmatrix}_j-\omega^2\left([\Phi]_{j-1}^j\begin{Bmatrix}p\\q\end{Bmatrix}_{j-1}\right.\\&\left.+[\Phi]_{j+|1}^j\begin{Bmatrix}p\\q\end{Bmatrix}_{j+1}+[\Phi]_{j-N_R}^j\begin{Bmatrix}p\\q\end{Bmatrix}_{j-N_R}+[\Phi]_{j+N_R}^j\begin{Bmatrix}p\\q\end{Bmatrix}_{j+N_R}\right)-\gamma^2\left([\Psi]_{j-1}^j\begin{Bmatrix}p\\q\end{Bmatrix}_{j-1}\right.\\&\left.+[\Psi]_{j+1}^j\begin{Bmatrix}p\\q\end{Bmatrix}_{j+1}+[\Psi]_{j-N_R}^j\begin{Bmatrix}p\\q\end{Bmatrix}_{j-N_R}+[\Psi]_{j-N_R}^j\begin{Bmatrix}p\\q\end{Bmatrix}_{j+N_R}\right)=0,\end{aligned} \tag{13}$$

As derived previously in this study, the non-dimensional equations of motion for the periodically-arranged tube array considered in the present study can be described in concise form as

$$-\bar{\omega}^2[M]\{V\}+\gamma^2[K]\{V\}=0. \tag{14}$$

where

$$\{V\} = \left[\begin{Bmatrix} p \\ q \end{Bmatrix}_1^T, \begin{Bmatrix} p \\ q \end{Bmatrix}_2^T, \begin{Bmatrix} p \\ q \end{Bmatrix}_3^T, \cdots, \begin{Bmatrix} p \\ q \end{Bmatrix}_N^T \right]^T. \tag{15}$$

In Eq. (14), matrices $[M]$ and $[K]$ have the forms

$$[M] = \begin{bmatrix} [M]_1^* & 0 & 0 & 0 \\ 0 & \ddots & 0 & 0 \\ 0 & 0 & \ddots & 0 \\ 0 & 0 & 0 & [M]_{N_W}^* \end{bmatrix}_{N\times N}, \tag{16a}$$

$$[K] = \begin{bmatrix} [K]_1^* & 0 & 0 & 0 \\ 0 & \ddots & 0 & 0 \\ 0 & 0 & \ddots & 0 \\ 0 & 0 & 0 & [K]_{N_W}^* \end{bmatrix}_{N\times N}, \tag{16b}$$

where $[M]_s^*$ and $[K]_s^*$ denote the corresponding mass and stiffness matrices of the tubes in the sth row, respectively. From the equations above, it can be shown that matrices $[M]_1^*$ and $[K]_1^*$ have the forms

$$[M]_1^* = \begin{bmatrix} [m]_1 + [\Phi]_1^1 & [\Phi]_2^1 & [0] & \cdots & [0] & [\Phi]_{1+N_R}^1 & [0] & \cdots & [0] \\ [\Phi]_1^2 & [m]_2 + [\Lambda_2^2] & [\Phi]_3^2 & [0] & \cdots & [0] & [\Phi]_{2+N_R}^2 & [0] & \cdots & [0] \\ [0] & \cdots & \cdots & \cdots & & & \cdots & & \cdots \\ \cdots & \cdots & \cdots & \cdots & & & \cdots & & \cdots \\ \cdots & & \cdots & \cdots & & & \cdots & & \cdots \\ [0] & \cdots & \cdots & [0] & [\Phi]_{N_R-1}^{N_R} & [m]_{N_R} + [\Phi]_{N_R}^{N_R} & [0] & \cdots & [0] & [\Phi]_{2N_R}^{N_R} \end{bmatrix}, \tag{17a}$$

$$[K]_1^* = \begin{bmatrix} [k]_1 + [\Psi]_1^1 & [\Psi]_2^1 & [0] & \cdots & [0] & [\Psi]_{1+N_R}^1 & [0] & \cdots & [0] \\ [\Psi]_1^2 & [k]_2 + [\Psi_2^2] & [\Psi]_3^2 & [0] & \cdots & [0] & [\Psi]_{2+N_R}^2 & [0] & \cdots & [0] \\ [0] & \cdots & \cdots & \cdots & & & \cdots & & \cdots \\ \cdots & \cdots & \cdots & \cdots & & & \cdots & & \cdots \\ \cdots & & \cdots & \cdots & & & \cdots & & \cdots \\ [0] & \cdots & \cdots & [0] & [\Psi]_{N_R-1}^{N_R} & [k]_{N_R} + [\Psi]_{N_R}^{N_R} & [0] & \cdots & [0] & [\Psi]_{2N_R}^{N_R} \end{bmatrix}. \tag{17b}$$

For simplicity, the same comparison function is applied for all of the tubes in the system, i.e., $\phi_s^j(\bar{r}) \equiv \phi_s(\bar{r})$. Furthermore, the tubes are all assumed to have the same mass, i.e., $m_j = m$. The non-dimensional frequency $\bar{\omega}_n$ in Eq. (14), i.e., the natural frequency of the mistuned tube array, is defined as

$$\bar{\omega}_n = \omega_n \Big/ \sqrt{\frac{EI}{mL^4}} \quad \text{for} \quad n = 1, 2, \ldots \tag{18}$$

3. Numerical results and discussions

The current analysis considers a periodic structure, a cross-flow heat exchange system with 60 tubes periodically arranged in a bundle comprising 6 rows, as shown in Fig. 1. The tubes are assumed to have dimensions of $L = 381$ mm (15 in.), $D = 25.4$ mm (1 in.), and $b = 0.71$ mm (0.0279 in.) and are arranged in an array with a pitch-to-diameter ratio of 1.35. The average flow velocity is specified as $U = 0.05$ m/s. An assumption is made that the 35th tube has a wear defect near its central region. Note that the remaining tubes in the array

are all assumed to be in perfect structural condition. As discussed earlier, the local structural irregularity in the defected tube results in a loss of stiffness in the transverse direction. The disorder in the sth defected tube is defined as

$$\varepsilon_s = \frac{\overline{EI} - (EI)_s}{\overline{EI}} \times 100\%, \tag{19}$$

where $\overline{EI}$ is the stiffness of the original tube and $(EI)_s$ is the stiffness of the sth defected tube.

Fig. 3 shows the variation of natural frequencies of the perfect tube array system with or without considering the squeezed liquid film effect between tubes. The results reveal that when fluid is not introduced into the tube bundle, the natural frequencies of the periodic tube array are virtually identical. However, when a fluid coupling effect is generated by introducing either a stationary fluid or a moving fluid within the bundle, the natural frequencies of the system are no longer equal, but increase slightly at higher vibrational modes. Furthermore, it can be seen that the additional mass introduced by the fluid lowers the natural frequency of the system; particularly under cross-flow conditions. Fig. 4 illustrates the effect of modal localization on the natural frequencies of the heat exchange system. As shown, the local defect on the 35th tube results in a reduction of the lowest natural frequency of the system. As mentioned in Bendiksen (1987) and Wei and Pierre (1988) and Orgun and Tongue (1994), corresponding to the localization frequency has a localization mode. In this modal localization condition, not only the defected tube, but also the neighboring tubes vibrate strongly. Due to the weak nature of the fluid coupling between the individual tubes in the bundle, the entire vibration energy is confined to just these few tubes, and hence further wear of both the defected tubes and its neighbors may take place, especially for the defected tube. Fig. 5(a) and (b) illustrate the mode shapes in the tube bundle with and without the modal localization effect. Note that for convenience, only eleven of the tubes near the defected tube, the 35th tube, are shown. Fig. 5(a) shows that in the case where the tubes are all perfect tubes, i.e., modal localization does not occur, the system is characterized by a symmetrical mode pattern. However, when a disorder of $\varepsilon_{35} = 15\%$ is applied to the 35th tube, an amplitude peak is observed at the defected node, as shown in Fig. 5(b), indicative of the modal localization effect. The results indicate that the mode localization is possible in a periodic tube system with considering the coupling effect of flow fluid.

The modal localization effect in the current mistuned tube array can be further illustrated by analyzing the amplitude distribution pattern within the system. For simplicity, the distribution pattern is best described by considering the maximum amplitude $(\sqrt{(u_j)^2 + (v_j)^2})$ of the central region of the tubes. Fig. 6 shows the maximum amplitudes of tubes 33–38 for the case where tube 35 has a local wear defect. The enhanced amplitude peak of the defected tube provides clear evidence of modal localization. Furthermore, it can be seen that the

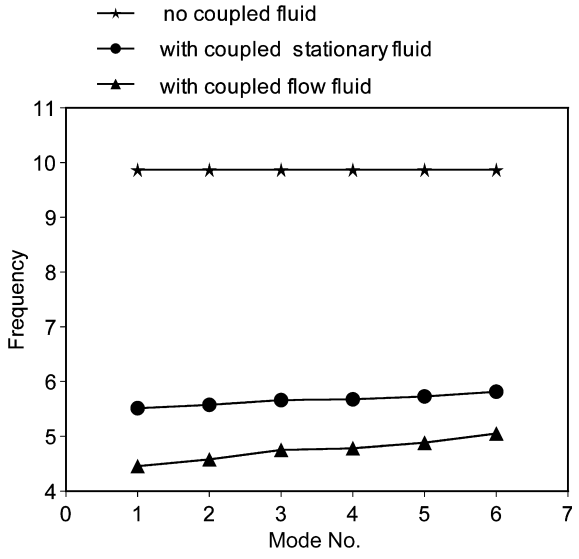

Fig. 3. Comparison of natural frequencies of tuned heat exchanger with and without fluid coupling effect.

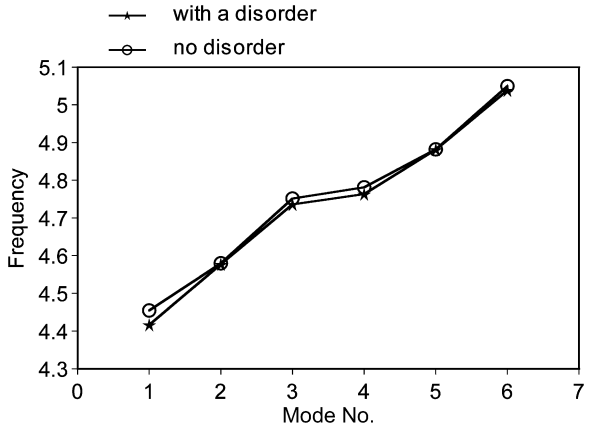

Fig. 4. Comparison of natural frequencies of heat exchanger in cross-flow with and without disorder.

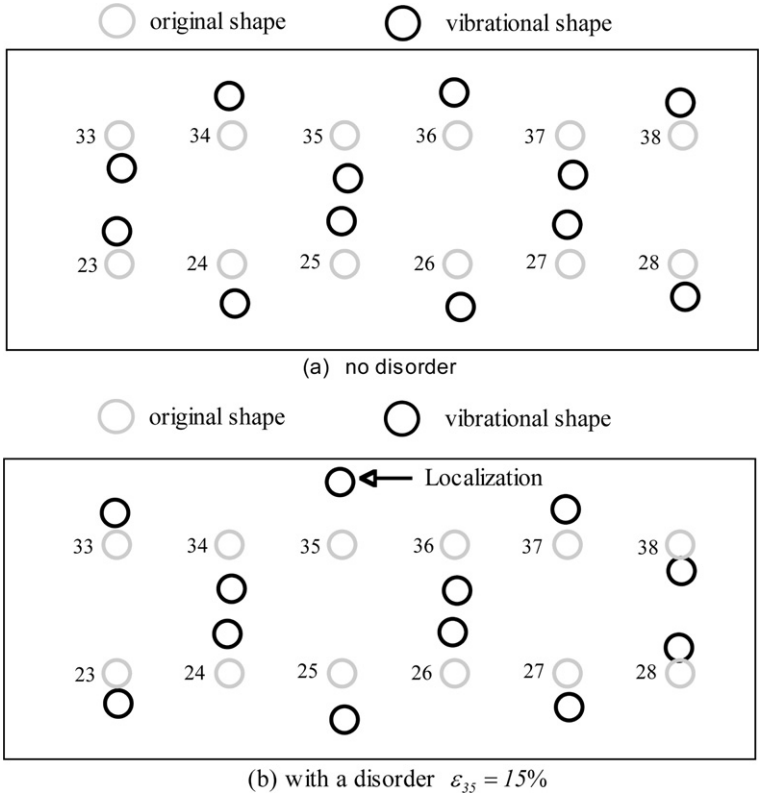

Fig. 5. Comparison of mode shapes of heat exchanger with and without disorder.

amplitude peaks of the neighboring tubes reduce rapidly with an increasing distance from the damaged tube, thus confirming that the vibrational energy induced by the defected tube is confined primarily to its immediate neighbors. Usually, this localized vibration pattern introduced from a local defect in a coupled periodic structure is called the localization mode. The simulated results show that the mode localization phenomenon is possible in a tube array with flow fluid. Fig. 7 illustrates the variation in the frequency response of a tuned and a mistuned tube bundle, respectively, when a uniformly distributed harmonic force of $\{\overline{F}\}e^{i\omega t}$ is applied to the tubes in the array. In the tuned system, the lowest natural frequencies are identical, and hence the frequency response contains only a single peak at $\bar{\omega} = 4.88$. However, in the mistuned system, the lower natural

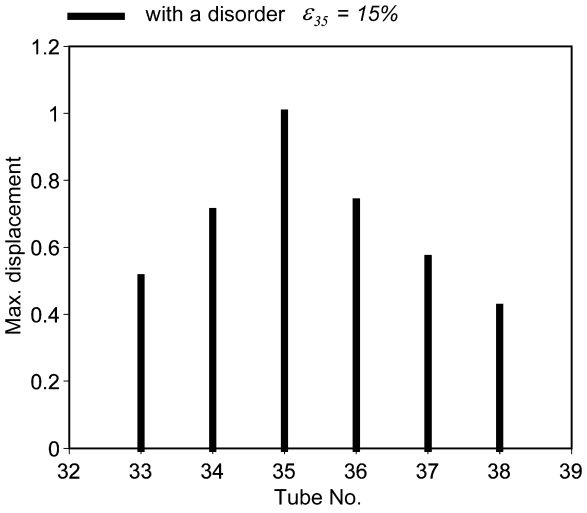

Fig. 6. Displacement pattern $|u_j(r,t)|$ of heat exchanger with disorder ($\varepsilon_{35} = 15\%$).

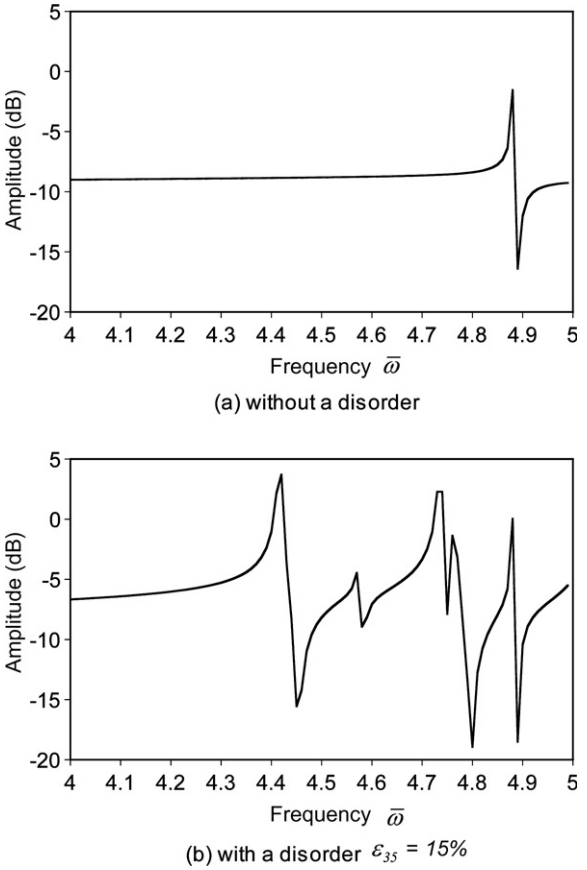

Fig. 7. Frequency responses of heat exchanger system with and without disorder ($\varepsilon_{35} = 15\%$).

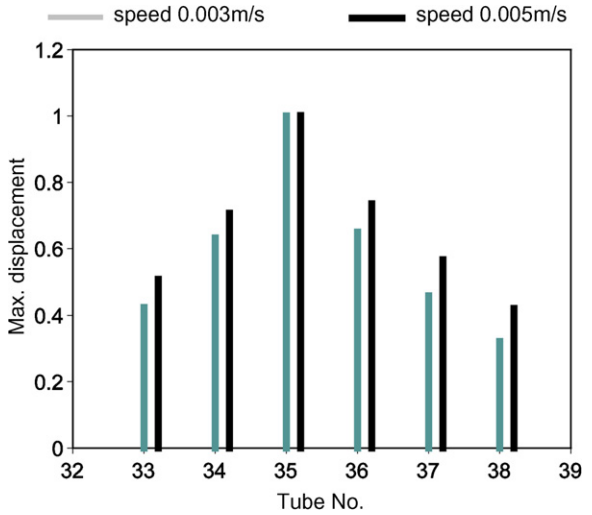

Fig. 8. Comparison of displacement patterns $|u_j(r,t)|$ in heat exchange system with different fluid flow speeds.

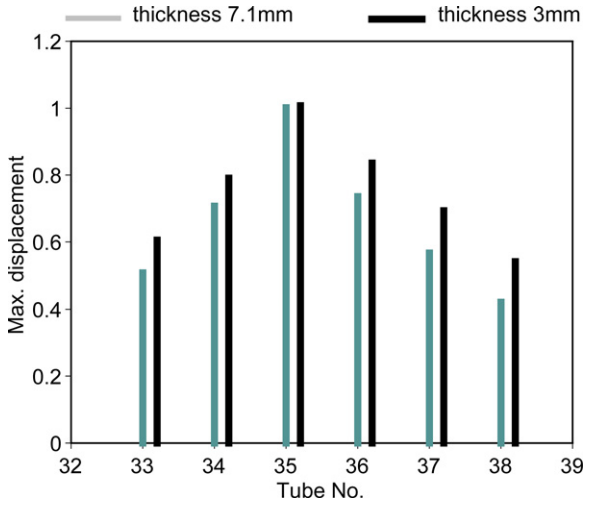

Fig. 9. Comparison of displacement patterns $|u_j(r,t)|$ in heat exchange system with different tube thicknesses.

frequencies are no longer the same, and thus a number of peaks are observed in the frequency response. From inspection, the lowest resonance frequency of the mistuned system, i.e., the localization frequency, is found to be $\bar{\omega}_1 = 4.4165$, which is close to, but lower than the lowest natural frequency of the tuned system.

Fig. 8 illustrates the effect of the fluid flow velocity on the localization mode pattern in a mistuned tube bundle. It is apparent that the mode pattern may vary from a strong localization to a weak localization as the fluid flow speed is increased. In other words, the fluid flow velocity may depress the mode localization vibration in the tube array system. Finally, Fig. 9 shows the effect of the tube thickness on the localization mode pattern in the mistuned system. From first principles, it is known that the tube stiffness increases as the wall thickness is increased. However, the results show that an increased tube thickness enhances the modal localization effect.

4. Conclusions

This study has performed a numerical investigation into the modal localization in a periodically-arranged, weakly-coupled tube array heat exchanger in cross-flow. The results support the following major conclusions:

(1) Local impact wear of even a single tube is sufficient to induce a severe vibration localization effect in a periodically-arranged tube bundle in cross-flow. Due to the weak coupling effect of the fluid between the individual tubes in the bundle, the vibrational energy induced by the modal localization effect is confined to the defected tube and to the tubes in its immediate vicinity.
(2) A higher flow rate suppresses the severity of the localization-induced vibrations. Conversely, the modal localization becomes more pronounced as the tube wall thickness is increased.
(3) The local disorder in a periodic tube structure may change the frequency response of the defected tube. A group of peak amplitudes spread in a wider frequency range is found for the defected tube, which is different from the single peak for a regular tube.

Acknowledgements

The author thank the National Science Council, Taiwan, Republic of China, for financially supporting this research project under Grant NSC 91-2212-E-230-001.

References

Bendiksen, O.O., 1987. Modal localization phenomena in large space structures. AIAA Journal 25, 1241–1248.
Eisinger, F.L., Francis, J.T., Sullivan, R.E., 1996. Prediction of acoustic vibration in steam generator and heat exchanger tube banks. ASME, Journal of Pressure Vessel Technology 118 (2), 221–236.
Huang, B.W., Kuang, J.H., 2001. Mode localization in a rotating mistuned turbo disk with coriolis effect. International Journal of Mechanical Science 43 (7), 1643–1660.
Katinas, V., Perednis, E., 1991. Crossflow-induced vibrations of staggered bundles of finned tubes. Fluid Mechanics 20 (3), 80–88.
Kuang, J.H., Huang, B.W., 1999. Mode localization on a cracked bladed disk. ASME, Journal of Engineering for Gas Turbine and Power (2), 335–342.
Kuang, J.H., Tsai, Y.C., 1987. A study on the Vibration of Cooling Water Heat Exchangers (I). In: Proceedings of the Atomic Energy Council Technical Report, Taipei, Taiwan. (in Chinese).
Kuang, J.H., Tsai, Y.C., 1988. A study on the Vibration of Cooling Water Heat Exchangers (II). In: Proceedings of the Atomic Energy Council Technical Report, Taipei, Taiwan. (in Chinese).
Kwak, K.M., Torii, K., Nishino, K., 2002. Heat transfer enhancement and pressure-loss reduction for fin-surfaces of in-line tube bundle with a single front row of winglet pairs. JSME International Journal, Series B: Fluids and Thermal Engineering 45 (4), 910–916.
Longatte, E., Benddjedou, Z., Souli, M., 2003. Methods for numerical study of tube bundle vibrations in cross-flows. Journal of Fluids and Structures 18 (5), 513–528.
Lorenzini, E., Giuliani, E., 2002. Dynamics of a tubular heat exchanger with arbitrary flow perturbation. Numerical Heat Transfer 42 (8), 833–854.
Orgun, C.O., Tongue, B.H., 1994. Modal localization in coupled circular plates. ASME Journal of Vibration and Acoustics 116, 286–294.
Papp, L., Chen, S.S., 1994. Turbulence-induced vibration of tube arrays in two-phase flow. ASME, Journal of Pressure Vessel Technology 116 (3), 312–316.
Price, S.J., Paidoussis, P., Macdonald, R., Mark, B., 1987. The flow-induced vibration of a single flexible cylinder in a rotated square array of rigid cylinders with pitch-to-diameter ratio of 2.12. Journal of Fluid and Structures 1, 359–378.
Taylor, C.E., Pettigrew, M.J., Dickinson, T.J., 1998. Vibration damping in multispan heat exchanger tubes. ASME, Journal of Pressure Vessel Technology (3), 283–289.
Weaver, D.S., Korogannakis, D., 1983. Flow-induced vibrations of heat exchanger u-tubes: a simulation to study the effects of asymmetric stiffness. Journal of Vibration, Acoustics Stress and Reliability 105, 67–124.
Weaver, D.S., Lover, J., 1977. Tube frequency effects on cross flow induced vibrations in tube arrays. In: Proceedings of the Fifth Biennial Symposium on Turbulence, Missouri, USA.
Wei, S.T., Pierre, C., 1988. Localization phenomena in mistuned assemblies with cyclic symmetry part I: free vibrations. ASME Journal of Vibration, Acoustics, Stress, and Reliability in Design 110, 429–438.
Yetisir, M., McKerrow, E., Pettigrew, M.J., 1998. Fretting wear damage of heat exchanger tubes: a proposed damage criterion based on tube vibration response. ASME, Journal of Pressure Vessel Technology 120 (3), 297–305.
Zhu, S., Chen, S.S., Cai, Y., 1997. Vibration and instability of two tubes in cross-flow. ASME, Journal of Pressure Vessel Technology 119, 142–149.
Zhu, S., Chen, S.S., Jendrzejczyk, J.A., 1994. Fluid damping and fluid stiffness of a tube row in cross-flow. ASME, Journal of Pressure Vessel Technology 116, 370–383.